Inorg. Chem. **2005**, *44*, 6071–6076

Charge Transport and Optical Properties of MOCVD-Derived Highly Transparent and Conductive Mg- and Sn-Doped In_2O_3 Thin Films

Jun Ni, Lian Wang, Yu Yang, He Yan, Shu Jin, and Tobin J. Marks*

Department of Chemistry and the Materials Research Center, Northwestern University, Evanston, Illinois 60208

John R. Ireland and Carl R. Kannewurf

Department of Electrical and Computer Engineering and the Materials Research Center, Northwestern University, Evanston, Illinois 60208

Received January 27, 2005

Mg- and Sn-doped In_2O_3 ($MgIn_xSn_yO_z$, $6.0 < x < 16.0$; $3.0 < y < 8.0$) thin films were grown by low-pressure metal-organic chemical vapor deposition using the volatile metal-organic precursors tris(2,2,6,6-tetramethyl-3,5-heptanedionato)indium(III) [In(dpm)$_3$], bis(2,4-pentanedionato)tin(II) [Sn(acac)$_2$], and bis(2,2,6,6-tetramethyl-3,5-heptanedionato)(*N*,*N*,*N*′,*N*′-tetramethylethylenediamine)magnesium(II) [Mg(dpm)$_2$(TMEDA)]. Films in this compositional range retain the cubic In_2O_3 bixbyite crystal structure. The highest conductivity is found to be ∼1000 S/cm for an as-grown film with a nominal composition $MgIn_{14.3}Sn_{6.93}O_z$. Annealing of such films in a vacuum raises the conductivity to ∼2000 S/cm. The optical transmission window of the present films is significantly wider than that of typical indium tin oxide (ITO) films from 300 to 3300 nm, and the transmittance is also greater than or comparable to that of commercial ITO films.

Introduction

Transparent conducting oxides (TCOs) have been the subject of intense research because of their importance in future display and photovoltaic technologies.[1,2] While Sn-doped In_2O_3 (ITO) is the most widely used TCO material, it has several limitations, such as relatively low transmission in the blue-green spectral region and suboptimal conductivity, which have stimulated a quest for ITO-alternative materials.

Since ITO and as-prepared In_2O_3[3,4] are both highly conductive and transparent, much of the research in this field has been directed at combining various transition and main-group metal oxides, such as ZnO,[5,6] CdO,[7,8] and MgO,[9−13] with In_2O_3 or ITO in order to find TCO materials with improved optical and electrical properties. Ueda et al. reported that bulk $MgIn_2O_4$ spinel is a wide band gap semiconductor with a conductivity as high as 100 S/cm.[10] It

* To whom correspondence should be addressed. E-mail: t-marks@northwestern.edu.

(1) Chopra, K. L.; Major, S.; Pandya, D. K. *Thin Solid Films* **1983**, *102*, 1.
(2) (a) Ohta, H.; Hosono, H. *Mater. Today* **2004**, *June*, 42. (b) Ginley, D. S.; Bright, C. *MRS Bulletin* **2000**, *8*, 15. (c) Granqvist, C. G. *Appl. Phys. A* **1991**, *52*, 83.
(3) Prince, J. J.; Ramamurthy, S.; Subramanian, B.; Sanjeeviraja, C.; Jayachandran, M. *J. Cryst. Growth* **2002**, *240*, 142.
(4) (a) Pan, C. A.; Ma, T. P. *J. Electrochem. Soc.* **1981**, *128*, 1953. (b) Taga, N.; Maekawa, M.; Shigesato, Y.; Yasui, I.; Kakei, M.; Haynes, T. E. *Jpn. J. Appl. Phys., Part 1* **1998**, *37*, 6524.
(5) (a) Wang, A. C.; Dai, J. Y.; Cheng, J. Z.; Chudzik, M. P.; Marks, T. J.; Chang, R. P. H.; Kannewurf, C. R. *Appl. Phys. Lett.* **1998**, *73*, 327. (b) Moriga, T.; Edwards, D. D.; Mason, T. O.; Palmer, G. B.; Poeppelmeier, K. R.; Schindler, J. L.; Kannewurf, C. R.; Nakabayashi, I. *J. Am. Ceram. Soc.* **1998**, *81*, 1310. (c) Phillips, J. M.; Cava, R. J.; Thomas, G. A.; Carter, S. A.; Kwo, J.; Siegrist, T.; Krajewski, J. J.; Marshall, J. H.; Peck, W. F.; Rapkine, D. H. *Appl. Phys. Lett.* **1995**, *67*, 2246.
(6) Palmer, G. B.; Poeppelmeier, K. R.; Mason, T. O. *Chem. Mater.* **1997**, *9*, 3121.
(7) (a) Wu, X.; Coutts, T. J.; Mulligan, W. P. *J. Vac. Sci. Technol., A* **1997**, *15*, 1057. (b) Shannon, R. D.; Gillson, J. L.; Bouchard, R. J. *J. Phys. Chem. Solids* **1977**, *38*, 877.
(8) Wang, A.; Babcock, J. R.; Edleman, N. L.; Metz, A. W.; Lane, M. A.; Asahi, R.; Dravid, V. P.; Kannewurf, C. R.; Freeman, A. J.; Marks, T. J. *Proc. Natl. Acad. Sci. U.S.A.* **2001**, *98*, 7113.
(9) Kanai, Y. *Jpn. J. Appl. Phys., Part 1* **1985**, *24*, L361.
(10) Ueda, N.; Omata, T.; Hikuma, N.; Ueda, K.; Mizoguchi, H.; Hashimoto, T.; Kawazoe, H. *Appl. Phys. Lett.* **1992**, *61*, 1954.
(11) Hosono, H.; Unno, H.; Ueda, N.; Kawazoe, H.; Matsunami, N.; Tanoue, H. *Nucl. Instrum. Methods Phys. Res., Sect. B* **1995**, *106*, 517.
(12) Minami, T.; Takata, S.; Kakumu, T.; Sonohara, H. *Thin Solid Films* **1995**, *270*, 22.
(13) Minami, T.; Miyata, T.; Yamamoto, T. *Surf. Coat. Technol.* **1998**, *109*, 583.

10.1021/ic0501364 CCC: $30.25
Published on Web 07/21/2005

has significantly greater optical transmission in the blue region (400−500 nm) than ITO. When co-deposited with $Zn_2In_2O_5$, the conductivity of sputtered films increases to ~1000 S/cm.[12] In addition, the work function and band gap of this material can be tailored by co-deposition with $Zn_2In_2O_5$ and $GaInO_3$.[13] Mg-doped In_2O_3 has also been studied, although the equilibrium solubility of Mg in In_2O_3 bulk materials is only ~0.5 cation %.[9,14] Such a small solubility does not provide a sufficiently large compositional range over which the electrical and optical properties of In_2O_3 can be significantly varied. To date, there has been no report on the effect of Sn doping in the Mg−In−O system, despite the general observation that Sn doping typically increases the carrier concentrations in In_2O_3- and CdO-based TCO materials, and hence conductivity. It has also been observed that doping Sn with Zn in In_2O_3 greatly increases the solubility of both species in In_2O_3.[6,15] This raises the interesting question whether similar solubility-increasing effects are applicable in the Mg−In−Sn−O (MITO) system.

Metal-organic chemical vapor deposition (MOCVD) is a growth technique widely used for compound semiconductor and oxide films. It offers advantages such as convenient compositional control, conformal film coverage, relatively simple equipment, and ready amenability to large area depositions. MOCVD also makes possible the growth of metastable phases that do not exist in standard phase diagrams,[8] which is a motivation for the present study.

In this contribution, we demonstrate the first effective low-pressure MOCVD film growth of Sn−Mg−In oxide films over a broad compositional range using tris(2,2,6,6-tetramethyl-3,5-heptanedionato)indium(III) [$In(dpm)_3$], bis(2,4-pentanedionato)tin(II) [$Sn(acac)_2$], and bis(2,2,6,6-tetramethyl-3,5-heptanedionato)(*N*,*N*,*N*′,*N*′-tetramethylethylenediamine)magnesium (II) [$Mg(dpm)_2$(TMEDA)] as precursors. Electrical and optical characterization reveals that such films are appreciably conductive, are highly transparent, and have broad transmission windows.

Experimental Section

General Synthetic Procedures. All glassware was rinsed with deionized water to minimize metal contamination. Standard Schlenk techniques and an M. Braun nitrogen-filled glovebox were used in the preparation of $Sn(acac)_2$. Tetrahydrofuran (THF) solvent was dried over NaK−benzophenone ketyl and distilled immediately prior to use. Pentane was passed through a dual-column (alumina and Q-5 copper catalyst) Solvtek solvent purification system. All other reagents were used as received.

Reagents and Physical Measurements. $Mg(NO_3)_2{\cdot}6H_2O$ (99.995% metal purity), $SnCl_2$ (anhydrous, 99.995% metal purity), and $In(NO_3)_3{\cdot}5H_2O$ (99.999% metal purity) were purchased from Alfa Aesar. The ligand reagent 2,2,6,6-tetramethyl-3,5-heptanedione (Hdpm; 99% purity) was purchased from Lancaster Synthesis and used as received. All other reagents were purchased from Aldrich. Commercial ITO films were purchased from Colorado Concept, LLC. Elemental analyses were performed by Midwest Microlabs, LLC. Melting points were determined in capillary tubes on a MelTemp melting point apparatus. NMR spectra were recorded on a Varian Mercury 400 MHz spectrometer.

Synthesis of Bis(2,2,6,6-tetramethyl-3,5-heptanedionato)-(*N*,*N*,*N*′,*N*′-tetramethylethylenediamine)magnesium(II), Mg(dpm)$_2$(TMEDA). This complex was synthesized by a modification of the literature procedure.[16] A three-neck, 1000 mL round-bottom flask equipped with a mechanical stirrer was charged with 34.00 g (0.133 mol) of $Mg(NO_3)_2{\cdot}6H_2O$, 60 mL of deionized H_2O, and 15.40 g (0.133 mol) of *N*,*N*,*N*′,*N*′-tetramethylethylenediamine. The resultant stirring solution was then treated with a suspension prepared by adding 48.83 g (0.266 mol) of Hdpm to 120 mL of a 0.5 M solution of NaOH in ethanol/water (3:1). A heavy white precipitate immediately formed. The resultant suspension was stirred for 3 h. The crude product was then collected on a glass frit and dried over P_4O_{10} in vacuo overnight. Pure $Mg(dpm)_2$(TMEDA) was obtained via sublimation (100 °C/10^{-4} Torr). Yield: 55.40 g (82.2%). mp: 213−215 °C. ^{1}H NMR (C_6D_6, δ): 1.24 [s, 36H, C(CH3)3], 2.17 [br s, 16H, $(CH_3)_2NH_2NH_2(CH_3)_2$], 5.73 (s, 2H, COCHCO). Anal. Calcd for $C_{28}H_{54}O_4N_2Mg$: C, 66.32; H, 10.73; N, 5.52. Found: C, 66.45; H, 10.76; N, 5.56.

Synthesis of Tris(2,2,6,6-tetramethyl-3,5-heptanedionato)-indium(III), In(dpm)$_3$. This complex was synthesized by a modification of the literature procedure.[17] A three-neck, 1000 mL round-bottom flask equipped with a mechanical stirrer was charged with 20.00 g (0.051 mol) of $In(NO_3)_3{\cdot}5H_2O$ and 180 mL of deionized H_2O. The resultant stirring solution was then treated with a solution prepared by adding 29.10 g (0.16 mol) of Hdpm dropwise into 400 mL of ethanol containing 9.34 g (0.16 mol) of 1-propylamine. A white precipitate immediately formed. The reaction mixture was stirred overnight. The crude product was then collected on a glass frit and dried over P_4O_{10} in vacuo overnight. Pure $In(dpm)_3$ was obtained via sublimation (130 °C/10^{-4} Torr). Yield: 26.32 g (77.4%). mp: 169−172 °C. Anal. Calcd for $C_{33}H_{57}O_6In$: C, 59.64; H, 8.64. Found: C, 59.25; H, 8.76. ^{1}H NMR (C_6D_6, δ): 1.19 (s, 54H, CH_3), 5.84 (s, 3H, COCHCO).

Synthesis of Bis(2,4-pentanedionato)tin(II), Sn(acac)$_2$. This complex was synthesized by a modification of the literature procedure.[18] Under a N_2 atmosphere, a two-neck, 500 mL round-bottom flask was charged with 15.37 g (0.081 mol) of anhydrous $SnCl_2$, 50 mL of freshly distilled THF, and 20.29 g (0.20 mol) of 2,4-pentanedione. To the stirring solution, 24.5 g (0.24 mol) of triethylamine was added dropwise via syringe. A white precipitate immediately formed. The reaction mixture was then refluxed under N_2 overnight. After cooling to room temperature, the THF was next removed in vacuo. Anhydrous pentane was added, and the suspension was filtered through a frit under N_2. The pentane was then removed in vacuo from the filtrate, and the remaining liquid was distilled under reduced pressure. The fraction of greenish-yellow, heavy liquid boiling at 95−105 °C/0.01 Torr was collected in a storage tube under N_2. Yield: 19.38 g (75.6%). bp: 94−96 °C/0.03 Torr. Anal. Calcd for $C_{10}H_{14}O_4In$: C, 37.90; H, 4.45. Found: C, 38.37; H, 4.59. ^{1}H NMR ($CDCl_3$, δ): 1.65 (s, 12H, CH_3), 5.07 (s, 2H, COCHCO).

Film Growth and Characterization. Corning 1737F glass substrates were first sonicated in high-purity acetone, then in hexane,

(14) Wakaki, M.; Yasuo, K. *Jpn. J. Appl. Phys.* **1986**, *25*, 502.
(15) Ni, J.; Yan, H.; Wang, A.; Yang, Y.; Stern, C. L.; Metz, A. W.; Jin, S.; Wang, L.; Marks, T. J.; Ireland, J.; Kannewurf, C. R. *J. Am. Chem. Soc.* **2005**, *127*, 5613.
(16) Babcock, J. R.; Benson, D. D.; Wang, A.; Edleman, N. L.; Belot, J. A.; Metz, A. W.; Marks, T. J. *Chem. Vap. Deposition* **2000**, *6*, 180.
(17) (a) Jablonski, Z.; Rychlowskahimmel, I.; Dyrek, M. *Spectrochim. Acta, Part A* **1979**, *35*, 1297. (b) Utsunomi, K. *Bull. Chem. Soc. Jpn.* **1971**, *44*, 2688.
(18) (a) Ewings, P. F. R.; Harrison, P. G.; Fenton, D. E. *J. Chem. Soc., Dalton Trans.* **1975**, 821. (b) Bos, K. D.; Budding, H. A.; Bulten, E. J.; Noltes, J. G. *Inorg. Nucl. Chem. Lett.* **1973**, *9*, 961.

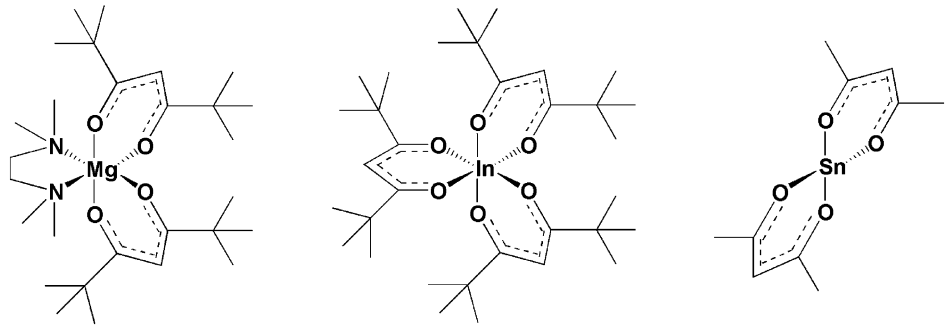

Figure 1. Mg, In, and Sn precursors used in the MOCVD growth of MITO thin films.

for 10 min each, prior to film growth. Sn−Mg−In−O (MITO) films were grown in the horizontal, low-pressure reactor as described elsewhere.[19] The optimized precursor temperatures and Ar carrier gas flow rates were $In(dpm)_3$, 105 °C/24 sccm; $Sn(acac)_2$, 25 °C/10−16 sccm; and $Mg(dpm)_2(TMEDA)$, 80 °C/8−10 sccm, with O_2 as an oxidizing gas flowing at 150−180 sccm. The system pressure was maintained at 3.0 ± 0.1 Torr, and the substrate temperature was optimized at 480 °C. Film growth rates are estimated to be ∼3 nm/min. Annealings of the as-grown films were performed in the same reactor in a vacuum (system pressure < 0.01 Torr). Film composition was analyzed using inductively coupled plasma atomic emission spectroscopy after the films were dissolved in hydrochloric acid. X-ray $\theta-2\theta$ scans (XRD) of the MOCVD-derived MITO films were performed on a Rigaku DMAX-A powder diffractometer using Ni-filtered Cu Kα radiation calibrated with Si powder sprinkled on the film surface. Room-temperature charge transport data were acquired on a Bio-Rad HL5500 Hall-effect measurement system, and variable-temperature measurements were recorded between 77 and 330 K using instrumentation described previously.[20] Optical transparency measurements were carried out on a Cary 500 UV−vis−NIR spectrometer from 300 to 3300 nm. The surface morphology of the MITO films was investigated on a Digital Instruments Nanoscope III atomic force microscope (AFM) operating in the contact mode. Film thickness was measured with a Tencor P-10 profilometer after etching a step in the film using hydrochloric acid. Refractive indices were measured on a Metricon 2010 prism coupler using a He−Ne laser (632.8 nm).

Results and Discussion

Film Growth and Microstructure Analysis. With $Mg(dpm)_2(TMEDA)$, $In(dpm)_3$, and $Sn(acac)_2$ used as precursors (Figure 1), MITO films were grown over a temperature range from 380 to 520 °C. The optimum deposition temperature window, in terms of phase purity, crystallinity, and morphology, was found, after some experimentation, to be from 460 to 480 °C. Below this range, deposited films either have heavy carbon contamination or are amorphous. Composition control was difficult for films deposited above this range because of precursor decomposition before reaching the deposition area. In general, higher temperatures yield lower carbon contamination and better crystallinity of the deposited films. Thus, 480 °C was chosen as the optimal growth temperature. MITO films were also grown at different oxygen flow rates in order to determine the optimal oxygen partial pressure in the reactor. While low oxygen partial pressure causes high carbon contamination in films because of incomplete precursor decomposition, high oxygen partial pressure leads to depressed film carrier concentrations and conductivities, which possibly results from a reduced oxygen vacancy concentration in the In_2O_3 structure. An oxygen partial pressure of 2.0−2.5 Torr was found to yield the most conductive and transparent films.

Films with the nominal composition $MgIn_xSn_yO_z$ ($6.0 < x < 17.0$; $3.0 < y < 8.0$) were grown on Corning 1737F glass substrates. In this compositional range, MITO films are found to have the bixbyite In_2O_3 crystal structure by XRD (Figure 2A). However, films with low In contents exhibit poorly crystalline microstructures and weak, broad reflections. When Mg and Sn reach the solubility limits in In_2O_3, MgO, SnO_2, or $MgIn_2O_4$ phases appear in the XRD patterns (Figure 2B). It is found that the introduction of Mg greatly enhances the solubility of Sn in In_2O_3, and the solubility limit of Sn in In_2O_3 is found to increase to ∼36 cation % in the MITO films grown in this study. In contrast, the solubility of Mg in bulk In_2O_3 materials was found to be below 1 cation %.[9,14] In the MITO films studied here, the solubility limit of Mg in In_2O_3 increases to ca. 10 cation %. Correspondingly, the lowest In content required for MITO films to retain the cubic In_2O_3 crystal structure is found to be ∼60 cation %, compared to ∼90 cation % for commercial ITO films. Thus, the coexistence of Mg and Sn significantly promotes the solubility of both species in MOCVD-derived In_2O_3 films.

Five series of MITO thin films are discussed below. Within each series, the Mg/In ratio is held constant while the Sn/Mg ratio is varied. Furthermore, the Mg/In ratio is varied between series. Film morphology was analyzed by contact mode AFM. Typical MOCVD-derived films are smooth with root-mean-square roughnesses of 5−6 nm for 300-nm-thick films. The films have densely packed grain structures with grain sizes varying from 50 to 200 nm, confirmed by both AFM and SEM.

Charge Transport Measurements. Four-probe conductivity measurements on the MOCVD-derived $MgIn_xSn_yO_z$

(19) Hinds, B. J.; McNeely, R. J.; Studebaker, D. B.; Marks, T. J.; Hogan, T. P.; Schindler, J. L.; Kannewurf, C. R.; Zhang, X. F.; Miller, D. J. *J. Mater. Res.* **1997**, *12*, 1214.
(20) Lyding, J. W.; Marcy, H. O.; Marks, T. J.; Kannewurf, C. R. *IEEE Trans. Instrum. Meas.* **1988**, *37*, 76.

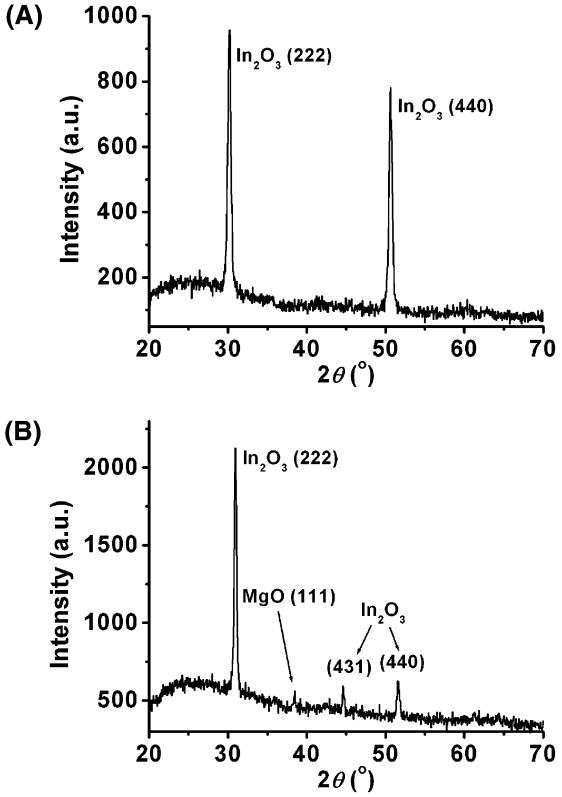

Figure 2. (A) $\theta-2\theta$ X-ray diffraction scan of a MOCVD-derived $MgIn_{16.1}Sn_{4.11}O_z$ film, showing the predominant In_2O_3 crystal structure. (B) $\theta-2\theta$ X-ray diffraction scan of a $MgIn_{6.90}Sn_{4.10}O_z$ film, showing both doped In_2O_3 and MgO phases [note the MgO (111) reflection at 38.5°].

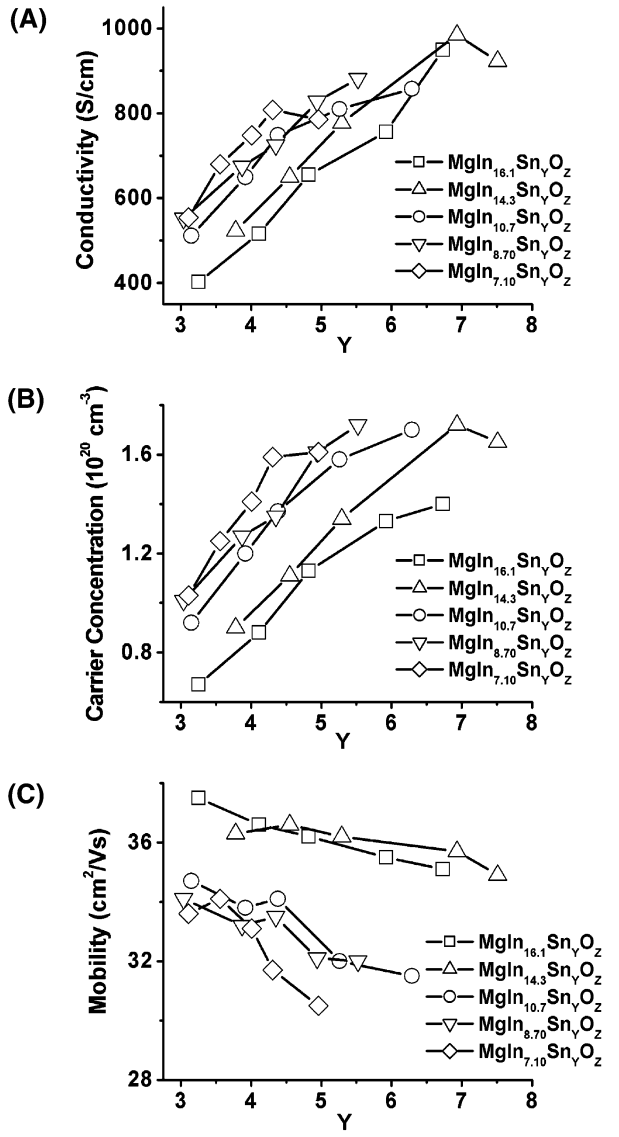

Figure 3. Room-temperature (A) conductivity-composition, (B) carrier concentration-composition, and (C) carrier mobility-composition plots for the MITO films. Lines through the data points are drawn as a guide for the eyes.

films over the aforementioned compositional range show that the electrical properties of these films are closely related to their chemical compositions. Room-temperature charge transport properties of MITO films as a function of chemical composition are plotted in Figure 3. Detailed data are compiled in Table S1 in the Supporting Information. Room-temperature Hall mobilities range from 30 to 40 cm^2/Vs, comparable to or greater than those of commercial polycrystalline ITO films, while carrier concentrations are on the order of 1×10^{20} cm^{-3}. In the series $MgIn_{7.10}Sn_yO_z$ and $MgIn_{14.3}Sn_yO_z$, both conductivity and carrier concentration first increase with increasing Sn content, then decrease after reaching a maximum. In the other three series, conductivity and carrier concentration increase with the Sn content until Sn reaches the solubility limit in In_2O_3. For all five series, carrier mobility generally decreases with increasing Sn and Mg content. All the films are significantly conductive, with conductivities invariably greater than 400 S/cm. All films show n-type transport, meaning that the majority of carriers are electrons. The highest conductivity is found to be 985 S/cm for an as-grown $MgIn_{14.3}Sn_{6.93}O_z$ film, with a mobility of 35.7 cm^2/Vs and a carrier concentration of 1.72×10^{20} cm^{-3}. While the mobility of $MgIn_{14.3}Sn_{6.93}O_z$ is comparable to that of commercial ITO, the carrier concentration is much lower than the $8-10 \times 10^{20}$ cm^{-3} value typically found in commercial ITO films.

Variable-temperature charge transport measurements on a $MgIn_{14.3}Sn_{6.93}O_z$ film reveal modest metal-like ($d\sigma/dT < 0$) charge transport behavior (Figure 4). The mobility decreases slightly with increasing temperature while the carrier concentration remains essentially constant, resulting in a slight decrease in conductivity from 78 K to room temperature. The dependence of mobility on temperature can be roughly divided into two regimes here: one below 160 K where mobility is essentially independent of temperature ($\mu \propto T^{-0.03}$) and one above 160 K where mobility temperature dependence increases to $\mu \propto T^{-0.29}$.

Optical Properties. Films with a thickness of ~300 nm exhibit an average transmittance greater than 85% in the visible range. The transparency extends well into the near-IR range, where all films exhibit >80% transmittance at 1500 nm. Figure 5 presents the UV−vis−NIR spectrum of a $MgIn_{14.3}Sn_{6.93}O_z$ film, which has the highest conductivity in the MITO series, and for a commercial ITO film. Transmission is calibrated versus uncoated glass substrates. The $MgIn_{14.3}Sn_{6.93}O_z$ film is more transparent than the ITO film throughout the wavelength measured, except in the UV

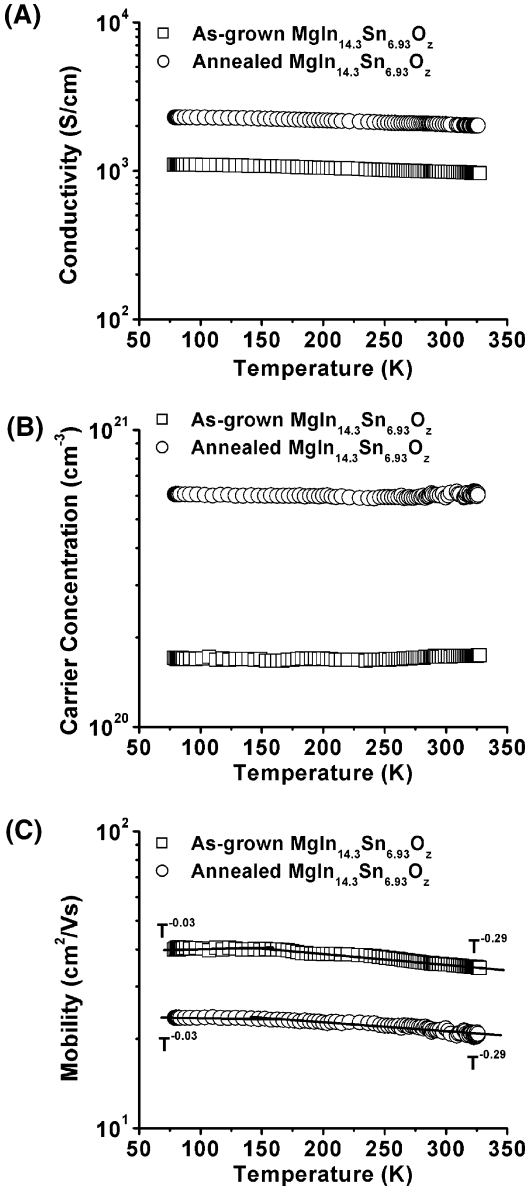

Figure 4. Variable-temperature charge transport measurements on a typical MOCVD-derived MITO ($MgIn_{14.3}Sn_{6.93}O_z$) film before and after annealing in a vacuum at 500 °C for 1.5 h.

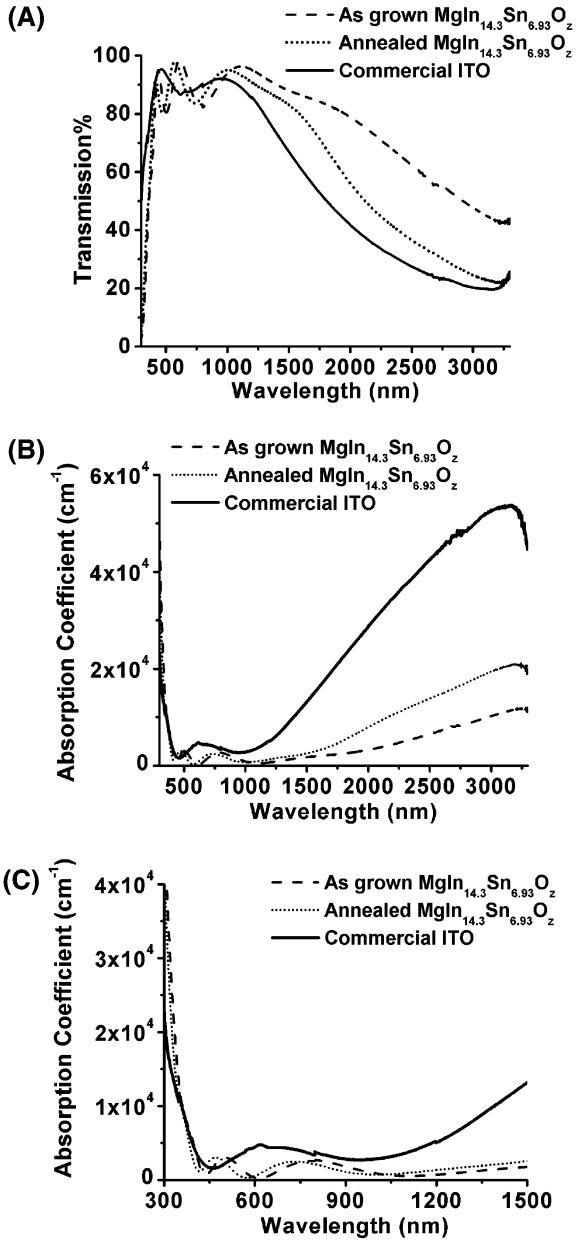

Figure 5. (A) UV−vis−NIR spectra of an as-grown $MgIn_{14.3}Sn_{6.93}O_z$ film, an annealed $MgIn_{14.3}Sn_{6.93}O_z$ film, and a commercial ITO film. (B) Corresponding absorption coefficients as a function of wavelength plot. (C) Enlargement of B from 300 to 1500 nm.

region. Note that $MgIn_{14.3}Sn_{6.93}O_z$ has far greater transmission in the NIR region than commercial ITO films. This high transmission in the NIR region is also observed in undoped SnO_2[1,21] and In_2O_3[3,22] films having similar carrier concentrations but considerably lower conductivities. The plasmon edge in the NIR region, arising from the absorption/reflection of free carriers, is significantly shifted toward longer wavelengths in $MgIn_{14.3}Sn_{6.93}O_z$ because of the relatively low carrier concentration, The band gap of $MgIn_{14.3}Sn_{6.93}O_z$, estimated from plotting $(\alpha h\nu)^2$ versus photon energy and assuming a direct band gap,[23] is 3.8 eV, falling within the 3.7−4.2 eV range reported for ITO films. The refractive index of $MgIn_{14.3}Sn_{6.93}O_z$ is 1.85 at 632 nm, significantly lower than the typical value of ∼2.0 for ITO thin films.[24]

Annealing Studies. Annealing of as-grown MITO films in a vacuum increases the conductivity by 70−110%, depending on the composition of the films. The annealing conditions were optimized as 500 °C and 1.5 h. Prolonged annealing and higher temperature do not significantly increase the conductivity. Table 1 present charge transport data for a $MgIn_{14.3}Sn_{6.93}O_z$ film before and after annealing. The carrier mobility decreases from 35.7 cm^2/Vs to 21.1

(21) (a) Shanthi, E.; Dutta, V.; Banerjee, A.; Chopra, K. L. *J. Appl. Phys.* **1980**, *51*, 6243. (b) Demichelis, F.; Minetti-Mezzett, E.; Smurro, V.; Tagliaferro, A.; Tresso, E. *J. Phys. D: Appl. Phys.* **1985**, *18*, 1825.
(22) Wickersham, C. E.; Greene, J. E. *Phys. Status Solidi A* **1978**, *47*, 329.
(23) Metz, A. W.; Ireland, J. R.; Zheng, J. G.; Lobo, R. P. S. M.; Yang, Y.; Ni, J.; Stern, C. L.; Dravid, V. P.; Bontemps, N.; Kannewurf, C. R.; Poeppelmeier, K. R.; Marks, T. J. *J. Am. Chem. Soc.* **2004**, *126*, 8477.
(24) Fukarek, W.; Kersten, H. *J. Vac. Sci. Technol., A* **1994**, *12*, 523.

Table 1. Charge Transport Data for a $MgIn_{14.3}Sn_{6.93}O_z$ Film before and after Annealing in Vacuum at 500 °C for 1.5 h[a]

$MgIn_{14.3}Sn_{6.93}O_z$	σ_{298} (S/cm)	μ_{298} (cm^2/Vs)	n_{298} ($10^{20}cm^{-3}$)	band gap (eV)
as-grown	985	35.7	1.72	3.82
annealed	2060	21.1	6.08	3.87

[a] σ: conductivity. n: carrier concentration. μ: carrier mobility.

cm^2/Vs after annealing, while the carrier concentration increases more than 3-fold, from $1.72 \times 10^{20}cm^{-3}$ to $6.08 \times 10^{20}cm^{-3}$. The net result is an increase in conductivity from 985 S/cm^2 to 2065 S/cm^2. Variable-temperature charge transport data for the same film after annealing can be found in Figure 4. The plasmon edge of annealed $MgIn_{14.3}Sn_{6.93}O_z$ shifts slightly toward shorter wavelengths compared to that of the as-grown film. The transmittance of the annealed film remains almost the same as that of as-grown $MgIn_{14.3}Sn_{6.93}O_z$. The band gap of annealed $MgIn_{14.3}Sn_{6.93}O_z$ increases slightly to 3.87 eV from 3.82 eV for as-grown $MgIn_{14.3}Sn_{6.93}O_z$, consistent with the expected effect of the greater carrier density through a Burstein−Moss shift.[25]

In the MITO films discussed here, the largest carrier concentration achieved is 1.72×10^{20} cm^{-3} for an as-grown $MgIn_{14.3}Sn_{6.93}O_z$ film, which is ~5 times lower than the $8-10 \times 10^{20}$ cm^{-3} found in typical polycrystalline ITO thin films,[26] despite the much greater Sn content in the MITO thin films (ranging from 16 to 31 cation %) than that in typical ITO thin films (7−10 cation %). This abnormally low carrier concentration in MITO can be attributed to two factors. The first one is the electron-neutralizing effect of Mg doping. While each electrically active Sn atom contributes one electron to the conduction band, each electrically active Mg atom contributes one hole, effectively canceling out the contribution from Sn, hence, reducing the carrier concentration. However, since the Mg content in the MITO is less than 10 cation %, Mg doping alone cannot explain such a low carrier concentration. The second factor is the formation of neutral species that reduces the Sn doping efficiency, such as nonreducible $(Sn_2O_4)^x$ and reducible $(2Sn_{In}^{\bullet}O_i'')^x$,[27] in the In_2O_3 matrix. That annealing of as-grown $MgIn_{14.3}Sn_{6.93}O_z$ films leads to a more than 300% increase in carrier concentration strongly suggests that there is a large quantity of reducible $(2Sn_{In}^{\bullet}O_i'')^x$ associates, which, upon annealing, release O_2 and form electrically active $Sn_{In}^{\bullet}$ species (Scheme 1). The existence of large quantities of $(2Sn_{In}^{\bullet}O_i'')^x$ is also supported by the 40% decrease in carrier mobility after annealing of the $MgIn_{14.3}Sn_{6.93}O_z$ film. The newly formed $Sn_{In}^{\bullet}$ resulting from annealing may act as ionized impurity scattering centers and, thus, reduce carrier mobility.

Scheme 1

$$(2Sn_{In}^{\bullet}O_i'')^x \longrightarrow 1/2O_2\,(g) + 2Sn^{\bullet} + 2e'$$

Release of O_2 from neutral associates $(2Sn_{In}^{\bullet}O_i'')^x$ upon annealing in MITO.

For both as-grown and annealed $MgIn_{14.3}Sn_{6.93}O_z$ films, that carrier mobility is essentially independent of temperature ($\mu \propto T^{-0.04}$) below 160 K suggests that the temperature-dependent lattice vibration scattering mechanism has little effect on carrier mobility below 160 K. At temperatures above 160 K, that carrier mobility scales only weakly with temperature ($\mu \propto T^{-0.29}$) argues for the influence on carrier mobility of other temperature-independent mechanisms.

Conclusions

Transparent conductive Mg- and Sn-doped In_2O_3 films were grown over a wide composition range by low-pressure MOCVD. The deposited films retain the cubic In_2O_3 bixbyite structure. It is worth noting that the coexistence of Mg and Sn in these films is found to promote the solubility of both elements in In_2O_3 dramatically. The highest conductivity for as-grown films is 985 S/cm for a $MgIn_{14.3}Sn_{6.93}O_z$ film, with a carrier concentration of $1.72 \times 10^{20}cm^{-3}$ and a carrier mobility of 35.7 cm^2/Vs. Annealing of the film in a vacuum increases the conductivity to 2060 S/cm because of a dramatic increase in carrier concentration. The transmittance and transparency window of the annealed films remain almost unchanged. While the conductivity of a $MgIn_{14.3}Sn_{6.93}O_z$ film, the composition of greatest conductivity, is somewhat less than that of typical ITO films, the transparency window and transmittance of the films are considerably greater. In particular, the high transmittance of $MgIn_{14.3}Sn_{6.93}O_z$ in the near-IR range makes it a promising material for near-IR optoelectronic applications.

Acknowledgment. We thank the U.S. Display Consortium (USDC) and NSF (CHE-0201767) for support of this research. We thank the Northwestern Materials Research Center (NSF MRSEC DMR-0076097) for providing characterization facilities.

Supporting Information Available: Detailed electrical and optical data of the MITO films. This material is available free of charge via the Internet at http://pubs.acs.org.

IC0501364

(25) Hamberg, I.; Granqvist, C. G. *J. Appl. Phys.* **1986**, *60*, R123.
(26) (a) Kim, H.; Pique, A.; Horwitz, J. S.; Mattoussi, H.; Murata, H.; Kafafi, Z. H.; Chrisey, D. B. *Appl. Phys. Lett.* **1999**, *74*, 3444. (b) Tahar, R. B. H.; Ban, T.; Ohya, Y.; Takahashi, Y. *J. Appl. Phys.* **1998**, *83*, 2631.
(27) Hwang, J. H.; Edwards, D. D.; Kammler, D. R.; Mason, T. O. *Solid State Ionics* **2000**, *129*, 135.